Fullerenes

DOI: 10.1002/anie.201108551

Rock-Salt-Type Crystal of Thermally Contracted C_{60} with Encapsulated Lithium Cation**

Shinobu Aoyagi, Yuki Sado, Eiji Nishibori, Hiroshi Sawa, Hiroshi Okada, Hiromi Tobita, Yasuhiko Kasama, Ryo Kitaura, and Hisanori Shinohara*

Metallofullerenes encapsulating metal atoms within the hollow carbon cage are promising materials for molecular devices such as a single molecular memory.[1,2] However, the yield of metallofullerenes is usually extremely low.[3] Recently, the macroscopic synthesis and complete isolation of metallofullerenes encapsulating a lithium cation, $Li^+@C_{60}$, have been achieved by the present group.[4] The cationic $Li^+@C_{60}$ has a high tendency to form ion-pair states with an anion such as $SbCl_6^-$. The electrostatic attraction between Li^+ and anions through the cage suggests an external control of the position and thermal motion of Li^+ inside the cage by the species and arrangement of anions outside the cage. The molecular arrangement and endohedral structure of $Li^+@C_{60}$ in the ionic crystals could be changed by replacing the anion.

The rock-salt (Na^+Cl^-) structure is one of the most well-known and stable structures for ionic crystals, in which a cation (Na^+) is octahedrally coordinated by six anions (Cl^-). A rock-salt-type $Li^+@C_{60}$ crystal could also be produced by pairing with adequate anions. In fact, a rock-salt-type hollow C_{60} crystal has been found in alkali-metal-doped fullerenes, MC_{60} (M = K, Rb, or Cs), wherein cations (M) occupy octahedral voids of the face-centered-cubic (fcc) lattice of freely rotating C_{60} anions at high temperature.[5]

Herein we report the synthesis and crystal structure analysis of the cationic metallofullerene rock salt $[Li^+@C_{60}](PF_6)^-$. The detailed molecular structure of the cation, $Li^+@C_{60}$, octahedrally coordinated by six PF_6^- anions is revealed by means of the synchrotron radiation (SR) X-ray diffraction (XRD) at SPring-8 (Hyogo, Japan).

The crystal structure of $[Li^+@C_{60}](PF_6)^-$ at 400 K is shown in the inset of Figure 1. The anions, PF_6^-, having a disordered

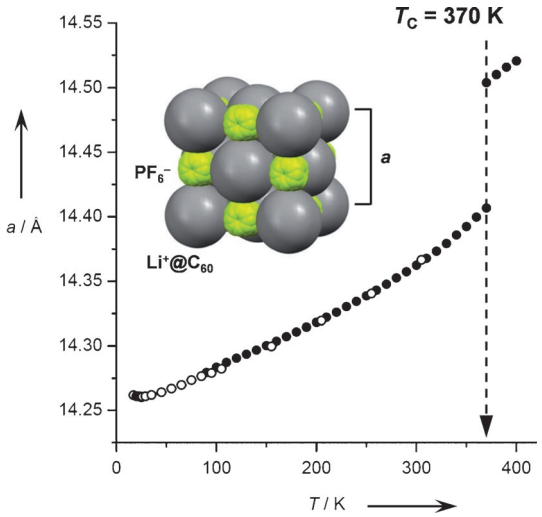

Figure 1. Temperature dependence of the lattice constant of $[Li^+@C_{60}](PF_6)^-$ measured for the single crystal (open circle) and powder sample (solid circle). The inset is the rock-salt-type fcc structure at a temperature above the T_C value.

orientation just fit into the octahedral voids of the fcc lattice of the almost freely rotating cations, $Li^+@C_{60}$, in the structure.[6] The fcc structure of rotating C_{60} cages is similar to that of pristine C_{60} at 300 K.[7] The crystal is the first example of a cationic metallofullerene crystal having symmetry (space group: $Fm\bar{3}m$) that is exactly the same as that of the rock salt.

The rotating $Li^+@C_{60}$ can be modeled by a uniform double spherical shell centered on the 4*a* sites at 0, 0, 0. The refined radii of the outer shell for C_{60} and inner shell for Li^+ are 3.548(1) and 1.3(1) Å, respectively. The rotational motion is regarded as a hindered rotation rather than a free rotation from the charge-density distribution obtained by the maximum entropy method (MEM; see Figure S5a in the Supporting Information). The charge density is not uniform for each shell. The charge density on the C_{60} shell is increased and decreased in the ⟨111⟩ and ⟨100⟩ directions, respectively (see Figure S5b). The non-uniform charge-density distribution which demonstrates the hindered rotation of C_{60} is different

[*] Dr. S. Aoyagi
Department of Information and Biological Science
Nagoya City University, Nagoya 467-8501 (Japan)
E-mail: aoyagi@nsc.nagoya-cu.ac.jp
Y. Sado, Dr. R. Kitaura, Prof. H. Shinohara
Department of Chemistry and Institute for Advanced Research
Nagoya University, Nagoya 464-8602 (Japan)
Dr. E. Nishibori, Prof. H. Sawa
Department of Applied Physics
Nagoya University, Nagoya 464-8603 (Japan)
Dr. H. Okada, Prof. H. Tobita
Department of Chemistry, Graduate School of Science
Tohoku University, Sendai 980-8578 (Japan)
Dr. Y. Kasama
Idea International Corporation
6-6-04, Aoba, Aramaki, Aoba-ku, Sendai 980-8579 (Japan)

[**] This work was supported by a Grant-in-Aid for Scientific Research from the MEXT of Japan (Grant Nos. 20360006 and 19051015). The synchrotron radiation experiments were performed at SPring-8 with approval of the Japan Synchrotron Radiation Research Institute (JASRI). We are grateful to Drs. K. Sugimoto and N. Yasuda for their help in the synchrotron radiation experiments.

Supporting information for this article is available on the WWW under http://dx.doi.org/10.1002/anie.201108551.

from the atomic-density distribution of pristine C_{60} as it decreases in the ⟨111⟩ direction,[8] but similar to that of C_{60} in Li_2CsC_{60}.[9] In contrast, the charge density on the Li^+ shell is increased in the ⟨100⟩ direction (see Figure S5c). This result demonstrates that an attractive interaction exists between Li^+ and PF_6^-, whereas a repulsive interaction exists between the carbon atoms and the Li^+ and/or PF_6^-.

PF_6^- anions having a disordered orientation can be modeled by a P atom on the 4*b* sites at 1/2, 1/2, 1/2, and partially occupied F atoms on the 48*i* sites at $1/2+\delta_1$, $1/2+\delta_1$, 1/2, and 96*k* sites at $1/2+\delta_2$, $1/2-\delta_2$, $1/2+\delta_3$ with the site occupancy of 1/6. The restricted rotational motion may be due to the concave shape of the voids surrounded by rotating $Li^+@C_{60}$ cations. The PF_6^- anions have a concave face to match the convex face of the adjacent rotating C_{60} cages (the inset of Figure 1 and Figure S5a). A similar "rotor-stator" molecular arrangement has been reported in the fullerene/cubane solid, $C_{60}{\cdot}C_8H_8$, in which static cubane molecules fill the octahedral voids of the fcc lattice of rotating C_{60}.[10]

The high-temperature fcc phase undergoes a phase transition to a low-temperature simple cubic (sc) phase at $T_C=370$ K with a jump in the lattice constant (Figure 1; see Figure S2 in the Supporting Information). The orientations of the C_{60} cages and PF_6^- are perfectly ordered in the sc phase (space group: $Pa\bar{3}$) at 300 K. A similar transition due to the ordering of the orientations is observed for pristine C_{60} and the hydrogen-encapsulating C_{60} $H_2@C_{60}$ at around 260 K.[7,11,12] The higher T_C value in $[Li^+@C_{60}](PF_6)^-$ suggests that an interaction preventing the C_{60} rotation exists. In contrast, decreases in the T_C value as a result of encapsulation of Ar and Kr have been reported for $Ar@C_{60}$ ($T_C=256$ K) and $Kr@C_{60}$ ($T_C=251$ K), respectively.[13]

The lattice constants of $[Li^+@C_{60}](PF_6)^-$ ($a=14.3666(4)$ Å at 300 K) are larger than those of pristine C_{60} ($a=14.17(1)$ Å at 300 K).[7] Such lattice expansion has also been reported for $Ar@C_{60}$.[13] The difference in the lattice constants between $Ar@C_{60}$ and pristine C_{60} is 0.002 Å at 300 K. The lattice expansion of $[Li^+@C_{60}](PF_6)^-$ is much greater than that of $Ar@C_{60}$, and mainly results from the filling of the octahedral voids with PF_6^-. A similar lattice expansion has been reported for $C_{60}{\cdot}C_8H_8$ ($a=14.74$ Å at 300 K),[10] whereas a lattice contraction has been reported for the rock-salt-type MC_{60} (M = K, $a=14.07$ Å at 473 K).[5] The lattice contraction in MC_{60} is due to an electrostatic attraction between M^+ and C_{60}^-. Such an electrostatic attraction between Li^+ and PF_6^- could also be present in $[Li^+@C_{60}](PF_6)^-$.

At a temperature below the T_C value, the orientation of C_{60} within $[Li^+@C_{60}](PF_6)^-$ is similar to the major of two orientations that coexist for pristine C_{60} even at 5 K;[11] the minor orientation is not observed in $[Li^+@C_{60}](PF_6)^-$. The C_{60} orientation can be represented by an angle, ϕ, which is an anticlockwise rotation about the [111] direction of an ideal molecular configuration with $Fm\bar{3}$ symmetry.[11] The angle $\phi=100.92(2)°$ for $[Li^+@C_{60}](PF_6)^-$ at 22 K is calculated from the refined atomic coordinates, and is slightly larger than that of for pristine C_{60} at 5 K ($\phi\approx98°$) as determined by the neutron powder diffraction.[11c]

The perfectly ordered C_{60} cages in $[Li^+@C_{60}](PF_6)^-$ enable us to determine the detailed cage structure. The radial distances of the ten independent carbon atoms from the cage center range from 3.5409(8) to 3.5556(9) Å at 22 K. The carbon atoms having the longer and shorter distances are oriented in the ⟨111⟩ and ⟨100⟩ directions, respectively.[6] The spherical C_{60} cage is, thus, slightly compressed along the unit-cell axes in $[Li^+@C_{60}](PF_6)^-$. The radial distances of carbon atoms are comparable with those for pristine C_{60} at 5 K which range from 3.541(5) to 3.556(6) Å within the experimental error.[11c]

The C_{60} cage radii, *r*, are estimated by averaging the radial distances of the carbon atoms and plotted against temperature (Figure 2). The cage radius for $[Li^+@C_{60}](PF_6)^-$ ($r=3.550(1)$ Å at 22 K) is also comparable with that for pristine C_{60} as determined by the neutron powder diffraction ($r=3.548(6)$ Å at 5 K) within the experimental error.[11c]

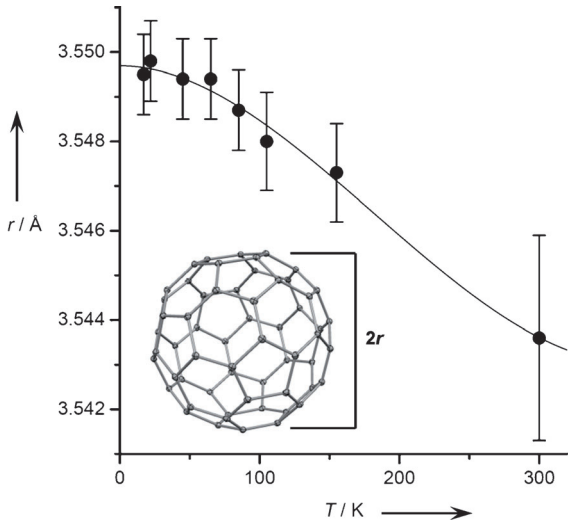

Figure 2. Temperature dependence of the C_{60} cage radius *r* of $[Li^+@C_{60}](PF_6)^-$ as estimated by averaging the radial distances of the carbon atoms from the cage center.

Although the experimental errors are not satisfactorily small to accurately detect the small changes of *r*, the negative thermal expansion (NTE) below 300 K can be seen in Figure 2. The NTE of C_{60} has been proposed on the basis of theoretical and experimental data.[14,15] The volumetric thermal expansion coefficient at around 100 K was estimated from the data in Figure 2 to be about -2×10^{-5} K^{-1}, a value larger than that predicted theoretically (-1×10^{-5} K^{-1}),[14] and smaller than that determined by EXAFS measurements of $Ar@C_{60}$ (-5×10^{-5} K^{-1}).[15] The NTE of C_{60} slightly elongates the C–C bond lengths. The temperature dependence of the C–C bond lengths are summarized in the Supporting Information.

Interestingly, the temperature dependence of the lattice constants given in Figure 1 and Figure S3 in the Supporting Information also show a small NTE at a temperature below 25 K. The usual positive thermal expansion of the lattice constant above 25 K is contrary to the NTE of the cage radius, and is mainly due to the increase of the intermolecular distance. The linear thermal expansion coefficients of the

lattice constant above 25 K is comparable with that for pristine C_{60} (see Figure S4).

In contrast to the static C_{60} cages, Li^+ cations are moving inside the cages. Our previous charge-density analysis of $[Li^+@C_{60}](SbCl_6)^-$ at 370 K using MEM clearly reconstructed charge-density peaks for one Li^+ inside the cage.[4] Nevertheless, no MEM charge-density peaks are found inside the cage of $[Li^+@C_{60}](PF_6)^-$ at 155 K (Figure 3a). To visualize the delocalized Li^+, model MEM charge densities calculated based on the refined structure model without any Li^+ are subtracted from the experimental values.

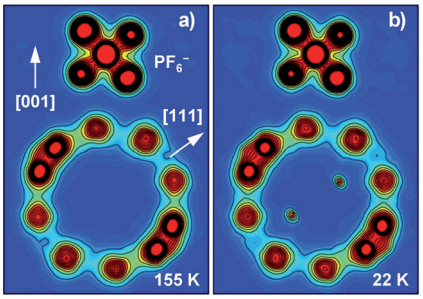

Figure 3. MEM charge-density maps of $[Li^+@C_{60}](PF_6)^-$ on the (1–10) plane at a) 155 and b) 22 K, respectively. The contour lines are drawn from 0 to 4.0 e Å^{-3} at intervals of 0.2 e Å^{-3}.

The equidensity surface of the difference-MEM charge densities at 0.015 e Å^{-3} inside the C_{60} cage at 155 K is shown as purple in Figure 4a. A shell-like positive difference-MEM charge density for the delocalized Li^+ is clearly found inside the C_{60} cage. The equidensity surface exhibits a dynamic or static positional disordering of Li^+ on the shell with a radius of about 1.5 Å. The shell-like charge densities are a little higher at near the centers of the six-membered rings, thus suggesting that Li^+ can occupy space under the twenty six-membered rings of the C_{60} cage. Remarkably, the Li^+ selectively occupies the positions with the highest charge densities (0.025 e Å^{-3}) under the eight six-membered rings around the threefold inversion axis. Four of these are shown as red sticks in Figure 4a. The other four are obtained by the inversion of these six-membered rings at the cage center.

The disordered Li^+ cations are gradually localized below 100 K without changes of the crystal symmetry. The MEM charge-density map and difference-MEM equidensity surface inside the cage at 22 K are shown in Figures 3b and 4b, respectively. The delocalized charge densities for Li^+ at 155 K are gradually condensed into two equivalent (crystallographic) positions within the C_{60} cage on the threefold inversion axis (8c sites at x, x, x) by decreasing the temperature (see also Figure S6 in the Supporting Information). The two positions having a charge density of 1.2 e Å^{-3} at 22 K are the most stable for Li^+ given the twenty possible positions beneath the six-membered rings. The Li^+ localization through decreasing the temperature implies that the disordered distribution of Li^+ over the twenty positions at 155 K (Figure 4a) is not static but rather a dynamic hopping, which is thermally excited. The thermal hopping of Li^+ is consistent with the ^{13}C NMR spectrum of $[Li^+@C_{60}](SbCl_6)^-$

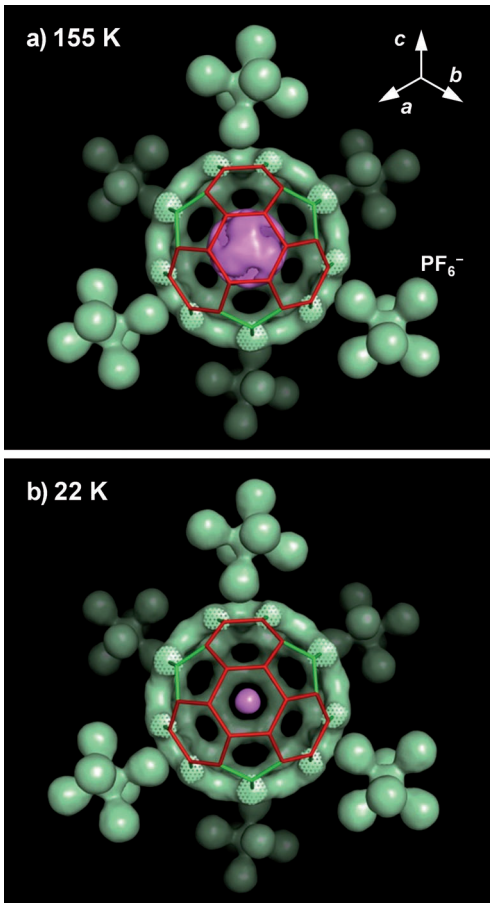

Figure 4. Equidensity surfaces of the difference-MEM charge densities for Li^+ (purple) at a) 155 K and b) 22 K as viewed from the [111] threefold inversion axis with the MEM charge densities (green). The purple surfaces represent difference-MEM charge densities inside the C_{60} cage at 0.015 and 0.100 e Å^{-3} in a) and b), respectively. The green surfaces represent MEM charge densities (not difference) at 1.0 e Å^{-3}, which are partially cut to show the inside of the C_{60} cage.

in solution which shows a single peak.[4] More detailed dynamics of Li^+ confined within a static C_{60} should be revealed by a solid NMR study of $[Li^+@C_{60}](PF_6)^-$.

The position and anisotropic atomic displacement parameters of Li^+ assumed at the 8c sites with the occupancy of 1/2 were refined.[6,16] The displacement of Li^+ from the cage center is 1.40(1) Å, which is close to the theoretical values.[17,18] The off-centered endohedral structure is common in mono-metallofullerenes,[3c,19] but is different from the centered structure of the nonmetal endohedral C_{60}.[12,13a,20] The nearest six-membered ring to Li^+ has three adjoined six-membered rings facing the coordinated PF_6^-. This arrangement tends to decrease the potential energy for Li^+ trapped under the six-membered rings (colored red in Figure 4) through the attractive Li–F electrostatic interaction. The symmetrical octahedral coordination of the PF_6^- anions around the C_{60} cage, on the other hand, should weaken the electrostatic potential on Li^+. As a result, the Li^+ cations in $[Li^+@C_{60}](PF_6)^-$ show a large thermal motion even at 155 K.

The attractive Li–F electrostatic interaction through the six-membered rings should prevent the rotational motion of

the C_{60} cage. The Li–F interaction increases the charge density of Li^+ within the vicinity of the PF_6^- anions at 155 K (Figure 4a), and also at 400 K above the T_C value (see Figure S5c in the Supporting Information). The electrostatic attraction between PF_6^- and Li^+ hopping among sites under twenty six-membered rings tends to fix the C_{60} orientation so that the six-membered rings face PF_6^-. The charge density on the C_{60} shell decreased in the ⟨100⟩ direction at 400 K (see Figure S5b) and can also be explained by the six-membered rings facing the PF_6^-. When the C_{60} cage is in the major and minor orientation of pristine C_{60}, the six- and five-membered rings are facing the PF_6^- anions. The fraction having the major orientation in pristine C_{60} can be expressed by using a Boltzmann distribution in which the energy difference between the major and minor orientations is 11.0 meV.[11b] The energy difference must be increased by the Li–F interaction, which prefers the major orientation in $[Li^+@C_{60}](PF_6)^-$. As a result, the major orientation is stabilized and C_{60} cages exhibits no disorder of orientation in $[Li^+@C_{60}](PF_6)^-$ at a temperature below the T_C value.

The substantially higher observed T_C value, relative to that of pristine C_{60}, could also be due to the Li–F interaction. The T_C value of pristine C_{60} increases with a lattice compression by pressure that increases the C_{60}–C_{60} interaction driving the ordering of the orientation.[21] Accordingly, the transition temperature should decrease with a lattice expansion. In fact, a decrease of the T_C value involving a lattice expansion has been reported for $C_{60}{\cdot}C_8H_8$ ($T_C = 140$ K) and $Ar@C_{60}$ ($T_C = 256$ K).[10,13] Importantly, the higher T_C value for $[Li^+@C_{60}](PF_6)^-$, involving the lattice expansion, is contrary to this effect. A similar increase of the T_C value involving a lattice expansion has been found in the Na-intercalated C_{60} $Na_{1.3}C_{60}$ ($T_C = 325$ K), wherein the electrostatic interaction between the C_{60} and Na^+ at the tetrahedral voids stabilizes the ordered phase.[22] The Li–F electrostatic attractive interaction which tends to fix the C_{60} orientation should stabilize the ordered phase for $[Li^+@C_{60}](PF_6)^-$. This interaction is one of the main reasons for the observed higher T_C value. The difference between the T_C values of $[Li^+@C_{60}](PF_6)^-$ ($T_C = 370$ K) and pristine C_{60} ($T_C = 260$ K) may correspond to the excitation energy needed for Li^+ to hop within the C_{60} cage.

The anisotropic thermal ellipsoids of the refined atomic displacement parameters for Li^+, at the two positions within the cage at 22 K, do not overlap with each other.[16] Thus, Li^+ occupying two positions within the cage at low temperature could not be explained by thermal hopping but rather by static disorder or tunneling. A static-disorder model for Li^+ is illustrated in Figure S10 in the Supporting Information. The Li^+ cations that were localized at either one of the two possible polar positions in the model can be explained by static disorder of the orientation of polar $Li^+@C_{60}$ cations. A theoretical tunneling model for the dynamics of Li within a C_{60} cage has been proposed.[18]

The crystal structure of the cationic metallofullerene rock salt $[Li^+@C_{60}](PF_6)^-$ reported here evidently demonstrates a strong interaction between Li^+, residing inside the C_{60} cage, and PF_6^- residing outside the cage; the interaction occurs through the six-membered rings. The interaction strongly restricts the rotational motion of the C_{60} cages. The detailed structure analysis of the perfectly ordered C_{60} cage at a temperature below the T_C value revealed a NTE and slight compression along the unit-cell axes. The Li^+ hops thermally inside the C_{60} cage even at 155 K, and is localized at the two polar positions at temperatures below 100 K because of the Li–F interaction. The orientation of the polar $Li^+@C_{60}$ cations at low temperature should be biased by applying an external electric field.[1] The external control of the molecular orientation and Li^+ position will be evaluated by dielectric measurements and X-ray structure analysis under an electric field.

Experimental Section

The high purity $[Li^+@C_{60}](PF_6)^-$ was obtained from $[Li^+@C_{60}](SbCl_6)^-$, which was synthesized by a previously reported method.[4,6] The anion replacement was performed by high-performance liquid chromatography (HPLC) using tetra-*n*-butylammonium hexafluorophosphate ($TBAPF_6$) as an electrolyte. The crystals of the resultant $[Li^+@C_{60}](PF_6)^-$ were grown by slow vaporization of the chlorobenzene/acetonitrile solution in a refrigerator.

The SR-XRD experiments for the $[Li^+@C_{60}](PF_6)^-$ crystals were carried out at SPring-8 (Hyogo, Japan).[6] The X-ray oscillation photographs of the single crystal were corrected by the large cylindrical imaging plate camera at BL02B1 beamline. The crystal structures at 17, 22, 45, 65, 85, 105, 155, 300 and 400 K were successfully determined with good reliability factors, i.e., $R1 = 0.0366$ (for $|F| > 3\sigma_F$, $d > 0.33$ Å) for 22 K.[6,16] The powder diffraction experiments of $[Li^+@C_{60}](PF_6)^-$ were also performed by the large Debye–Scherrer camera at BL02B2 beamline.

Received: December 5, 2011
Revised: January 20, 2012
Published online: February 28, 2012

Keywords: electrostatic interactions · fullerenes · lithium · molecular devices · phase transitions

[1] a) Y. Yasutake, Z. Shi, T. Okazaki, H. Shinohara, Y. Majima, *Nano Lett.* **2005**, *5*, 1057–1060; b) M. Iwamoto, D. Ogawa, Y. Yasutake, Y. Azuma, H. Umemoto, K. Ohashi, N. Izumi, H. Shinohara, Y. Majima, *J. Phys. Chem. C* **2010**, *114*, 14704–14709.
[2] C. J. Nuttall, Y. Hayashi, K. Yamazaki, T. Mitani, Y. Iwasa, *Adv. Mater.* **2002**, *14*, 293–296.
[3] a) K. Kikuchi, S. Suzuki, Y. Nakao, N. Nakahara, T. Wakabayashi, H. Shiromaru, K. Saito, I. Ikemoto, Y. Achiba, *Chem. Phys. Lett.* **1993**, *216*, 67–71; b) H. Shinohara, H. Yamaguchi, N. Hayashi, H. Sato, M. Ohkohchi, Y. Ando, Y. Saito, *J. Phys. Chem.* **1993**, *97*, 4259–4261; c) H. Shinohara, *Rep. Prog. Phys.* **2000**, *63*, 843–892.
[4] S. Aoyagi et al., *Nat. Chem.* **2010**, *2*, 678–683.
[5] Q. Zhu, O. Zhou, J. E. Fischer, A. R. McGhie, W. J. Romanow, R. M. Strongin, M. A. Cichy, A. B. Smith III, *Phys. Rev. B* **1993**, *47*, 13948–13951.
[6] For details, see the Supporting Information.
[7] a) P. A. Heiney, J. E. Fischer, A. R. McGhie, W. J. Romanow, A. M. Denenstein, J. P. McCauley, Jr., A. B. Smith III, D. E. Cox, *Phys. Rev. Lett.* **1991**, *66*, 2911–2914; b) P. A. Heiney, *J. Phys. Chem. Solids* **1992**, *53*, 1333–1352.
[8] P. C. Chow, X. Jiang, G. Reiter, P. Wochner, S. C. Moss, J. D. Axe, J. C. Hanson, R. K. McMullan, R. L. Meng, C. W. Chu, *Phys. Rev. Lett.* **1992**, *69*, 2943–2946.

[9] I. Hirosawa, K. Prassides, J. Mizuki, K. Tanigaki, M. Gevaert, A. Lappas, J. K. Cockcroft, *Science* **1994**, *264*, 1294 – 1297.
[10] a) S. Pekker et al., *Nat. Mater.* **2005**, *4*, 764 – 767; b) C. Bousige, S. Rols, J. Cambedouzou, B. Verberck, S. Pekker, É. Kováts, G. Durkó, I. Jalsovsky, É. Pellegrini, P. Launois, *Phys. Rev. B* **2010**, *82*, 195413; c) G. Bortel, S. Pekker, É. Kováts, *Cryst. Growth Des.* **2011**, *11*, 865 – 874.
[11] a) W. I. F. David, R. M. Ibberson, T. J. S. Dennis, J. P. Hare, K. Prassides, *Europhys. Lett.* **1992**, *18*, 219 – 225; b) W. I. F. David, R. M. Ibberson, T. Matsuo, *Proc. R. Soc. London Ser. A* **1993**, *442*, 129 – 146; c) W. I. F. David, R. M. Ibberson, J. C. Matthewman, K. Prassides, T. J. S. Dennis, J. P. Hare, H. W. Kroto, R. Taylor, D. R. M. Walton, *Nature* **1991**, *353*, 147 – 149.
[12] Y. Kohama et al., *Phys. Rev. Lett.* **2009**, *103*, 073001.
[13] a) K. Yakigaya et al., *New J. Chem.* **2007**, *31*, 973 – 979; b) A. Takeda et al., *Chem. Commun.* **2006**, 912 – 914.
[14] Y.-K. Kwon, S. Berber, D. Tománek, *Phys. Rev. Lett.* **2004**, *92*, 015901.
[15] a) N. Dragoe, A. M. Flank, P. Lagarde, S. Ito, H. Shimotani, H. Takagi, *Phys. Rev. B* **2011**, *84*, 155448; b) S. Brown, J. Cao, J. L. Musfeldt, N. Dragoe, F. Cimpoesu, S. Ito, H. Takagi, R. J. Cross, *Phys. Rev. B* **2006**, *73*, 125446.
[16] CCDC 853477 contains the supplementary crystallographic data for this paper. These data can be obtained free of charge from The Cambridge Crystallographic Data Centre via www.ccdc.cam.ac.uk/data_request/cif.
[17] Z. Slanina, F. Uhlík, S.-L. Lee, L. Adamowicz, S. Nagase, *Chem. Phys. Lett.* **2008**, *463*, 121 – 123.
[18] M. Zhang, L. B. Harding, S. K. Gray, S. A. Rice, *J. Phys. Chem. A* **2008**, *112*, 5478 – 5485.
[19] a) E. Nishibori, M. Takata, M. Sakata, H. Tanaka, M. Hasegawa, H. Shinohara, *Chem. Phys. Lett.* **2000**, *330*, 497 – 502; b) E. Nishibori, M. Takata, M. Sakata, M. Inakuma, H. Shinohara, *Chem. Phys. Lett.* **1998**, *298*, 79 – 84; c) M. Takata, B. Umeda, E. Nishibori, M. Sakata, Y. Saito, M. Ohono, H. Shinohara, *Nature* **1995**, *377*, 46 – 49.
[20] K. Kurotobi, Y. Murata, *Science* **2011**, *333*, 613 – 616.
[21] G. A. Samara, J. E. Schirber, B. Morosin, L. V. Hansen, D. Loy, A. P. Sylwester, *Phys. Rev. Lett.* **1991**, *67*, 3136 – 3139.
[22] T. Yildirim, J. E. Fischer, A. B. Harris, P. W. Stephens, D. Liu, L. Brard, R. M. Strongin, A. B. Smith III, *Phys. Rev. Lett.* **1993**, *71*, 1383 – 1386.

